[CANCER RESEARCH 60, 666–671, February 1, 2000]

Tumor-targeting Chemotherapy by a Xanthine Oxidase-Polymer Conjugate That Generates Oxygen-free Radicals in Tumor Tissue[1]

Tomohiro Sawa, Jun Wu, Takaaki Akaike, and Hiroshi Maeda[2]

Department of Microbiology, Kumamoto University School of Medicine, Kumamoto 860-0811, Japan

ABSTRACT

Xanthine oxidase (XO) mediates anticancer activity because of its ability to generate cytotoxic reactive oxygen species (ROS), including superoxide anion radical and hydrogen peroxide. However, the high binding affinity of XO to blood vessels would cause systemic vascular damage and hence limits the use of native XO in clinical settings. We demonstrate here that chemical conjugation of XO with poly(ethylene glycol) (PEG; the conjugates hereafter referred to as PEG-XO) significantly enhanced the tumor-targeting efficacy and the antitumor activity of XO. By using a succinimide-activated PEG derivative, PEG was conjugated to ε-amino groups of lysine residues of XO, which play a crucial role in binding of XO to blood vessels. PEG-XO administered i.v. showed a 2.8-fold higher accumulation in solid tumor compared with that of native XO 24 h after injection, whereas a slight or negligible increase in accumulation of PEG-XO was observed in normal organs. The highest PEG-XO enzyme activity was detected in tumor compared with normal organs or tissues except blood; enzyme activity in tumor was 5.0, 3.9, and 9.4 times higher than that in liver, kidney, and spleen, respectively. Intratumor activity remained high for >48 h. Administration of hypoxanthine, a substrate of XO, at 33 mg/kg body weight i.p. 12 h after the administration of PEG-XO (0.6 unit/mouse, i.v.) resulted in significant suppression of tumor growth ($P < 0.001$), with no tumor growth even after 52 days. However, either PEG-XO or hypoxanthine alone, or native XO with hypoxanthine, showed no effect on the inhibition of tumor growth under present experimental conditions. These findings suggest that PEG-XO, which accumulates preferentially in tumor tissue, warrants further investigation as a novel anticancer agent.

INTRODUCTION

XO[3] is an iron-containing metalloflavoprotein that catalyzes the two-step oxidation of purines, such as hypoxanthine, through xanthine, to uric acid. In this oxidation, molecular oxygen (O_2) is used as an electron acceptor; and hence, ROS including superoxide anion (O_2^-) and hydrogen peroxide (H_2O_2) are generated (1). It has been reported that XO showed antitumor activity (2, 3), probably via the generation of ROS. However, critical reevaluation of the antitumor effect of native XO showed that the results were variable and the efficacy was insignificant (4).

ROS generated from many antitumor drugs are known to exhibit antitumor effects on the basis of their highly cytotoxic nature. However, systemic distribution of these drugs causes undesirable side effects (5). For instance, native XO binds to blood vessels after administration into blood because of its high binding affinity for vascular endothelial cells (6–8). We anticipate that binding of XO to blood vessels would cause serious side effects, for example: (*a*) O_2^- generated from XO would oxidatively damage blood vessels; (*b*) the extremely rapid reaction of O_2^- with endogenously formed nitric oxide (NO), which dilates or maintains the vascular tone of blood vessels, would lower the level of NO in blood (8), thus resulting in elevation of blood pressure (9, 10). In addition, depletion of NO would cause vascular constriction and peripheral circulation insufficiency, which would result in necrosis or tissue degeneration; and (*c*) a reaction product of O_2^- and NO, peroxynitrite ($ONOO^-$), would further oxidatively damage blood vessels and other normal tissues or organs as well as tumor. Therefore, clinical use of native XO would be dangerous. Furthermore, endogenous anti-XO antibody may develop naturally if XO is not polymer conjugated, and it would reduce the activity of i.v.-injected XO in a week or two. The effect of a subsequent injection would be completely nullified, and thus XO would no longer be beneficial (11, 12).

To enhance the therapeutic efficacy of anticancer agents while reducing systemic side effects, it is necessary to deliver the drug (*e.g.*, XO) selectively to tumor tissue. We found previously that all biocompatible macromolecular drugs and lipids accumulate selectively in tumor tissue compared with other normal tissues and organs (13–15). In addition, they are retained in tumor tissue for a long time, *e.g.*, >100 h (13, 16). This phenomenon is referred to as the EPR effect of macromolecules and lipids in solid tumor. This EPR effect was validated in many experimental solid tumors, *e.g.*, Walker 256 carcinoma of the rat (17); VX-2 carcinoma of the rabbit (18, 19); sarcoma 180 (S-180; Refs. 13, 20–22) and B16 melanoma (20) of the mouse; and human hepatocellular carcinoma (23, 24). Very recently, a clinical trial of hydroxypropylmethacrylamide-copolymer conjugate with doxorubicin also demonstrated that this concept is valid (20, 25, 26). Therefore, we expect that if we could block the binding of XO to vascular endothelium (*e.g.*, by conjugating XO with PEG), more effective delivery of XO to tumor would be possible after conjugating XO with PEG, because of the EPR effect.

It has been reported that ε-amino groups of the lysine residues of XO play a crucial role in the binding of XO to vascular endothelial cells (6). Therefore, by masking lysine residues with a water-soluble biocompatible polymer, PEG, it would be possible to hinder the interaction between XO and endothelial cells. Consequently, we anticipated a high blood level of XO and its accumulation in tumor via the EPR effect. In this report, the synthesis, tumor accumulation, and antitumor effect of PEG-XO are described.

MATERIALS AND METHODS

Materials

XO (from bovine milk) and hypoxanthine were purchased from Sigma Chemical Co. (St. Louis, MO). Succinimidyl derivative of PEG propionic acid, which has an average molecular weight of M_r 5000, was obtained from Shearwater Polymers, Inc. (Huntsville, AL). $Na^{125}I$ was from ICN Pharmaceuticals, Inc. (Irvine, CA). Other reagents were of reagent grade and used without further purification.

Received 6/15/99; accepted 12/1/99.

The costs of publication of this article were defrayed in part by the payment of page charges. This article must therefore be hereby marked *advertisement* in accordance with 18 U.S.C. Section 1734 solely to indicate this fact.

[1] This work was supported by a grant from the Sagawa Foundation for Frontier Science and Technology, Kyoto (1997 and 1999).

[2] To whom requests for reprints should be addressed, at Department of Microbiology, Kumamoto University School of Medicine, 2-2-1 Honjo, Kumamoto 860-0811, Japan. Phone: 81-96-373-5098; Fax: 81-96-362-8362; E-mail: msmaedah@gpo.kumamoto-u.ac.jp.

[3] The abbreviations used are XO, xanthine oxidase; ROS, reactive oxygen species; PEG, poly(ethylene glycol); PEG-XO, PEG-conjugated XO; EPR, enhanced permeability and retention; TNBS, 2,4,6-trinitrobenzensulfonic acid; HO-1, heme oxygenase-1; FPLC, fast protein liquid chromatography.

Animals

Male ddY mice, 6 weeks of age, weighing 30–35 g (from SLC, Inc., Sizuoka, Japan), were used in this study. All experiments were carried out according to the guidelines of the Laboratory Protocol of Animal Handling, Kumamoto University School of Medicine.

Synthesis of PEG-XO

XO was subjected to ultrafiltration to remove ammonium sulfate and stabilizing agent such as salicylate with the use of an Amicon system (PM-30 membrane; cutoff size, M_r 30,000) before polymer conjugation. The concentration of the XO solution was adjusted to 10 mg/ml protein with 50 mM sodium phosphate buffer (pH 7.4). To the XO solution, succinimide-activated PEG was added at molar ratios of PEG per mol of lysyl ϵ-amino group of XO of 1.2 or 6.7, to prepare PEG-XO conjugates having low (PEG-XO-low) and high (PEG-XO-high) contents of PEG. Native XO is known to have 89 free ϵ-amino groups of lysine/mol plus one NH_2-terminal amino group. Unreacted PEG derivatives with functional groups, degradation products, and other impurities were removed by ultrafiltration using the PM-30 membrane as mentioned above. The conjugates thus obtained were stored in 50 mM sodium phosphate buffer (pH 7.4) containing 1 mM sodium salicylate for stabilization at 4°C.

Determination of the Degree of PEG Conjugation

The degree of PEG conjugation was determined by the loss of free amino groups as a result of PEG coupling. An amino group-specific reagent, TNBS was used to quantify the free amino groups of PEG-XO spectroscopically (27). Glycine was used as a standard. The protein concentrations of both native XO and PEG-XO conjugates were quantified by using the DC Protein Assay kit (Bio-Rad Laboratories, Hercules, CA). The molecular weights of these PEG-XO conjugates were estimated on the basis of the degree of conjugation, *i.e.,* loss of free amino groups as determined by the TNBS assay as well as approximation by the size exclusion elution profile described below.

Size Exclusion Chromatography

The increase in the molecular size of XO after PEG conjugation was confirmed by means of size exclusion chromatography using the FPLC system (Pharmacia LKB, Uppsala, Sweden) equipped with a Superose 6 HR 10/30 column (Pharmacia LKB), using the mobile phase of 50 mM sodium phosphate buffer (pH 7.4), and monitored by absorption at 280 nm.

Enzyme Activity of PEG-XO

Enzyme activity was determined by quantifying the formation of: (*a*) uric acid from xanthine by measuring the increase in absorbance at 290 nm, ϵ_{max} of uric acid (28); or (*b*) isoxanthopterin from pterin by measuring the increase in fluorescence emission at 390 nm, with excitation at 345 nm (29). The initial concentrations of the substrates were 0.05 and 0.01 mM for xanthine and pterin, respectively. The enzyme reaction was carried out in 50 mM sodium phosphate buffer (pH 7.4) at 25°C. One unit of XO activity is defined by the velocity of the formation of uric acid (μmol)/min.

In Vivo Distribution of PEG-XO after i.v. Injection

Radiolabeling and *in Vivo* Distribution of Radioactivity. *In vivo* distribution of native XO and PEG-XO-high (referring larger molecular size with more PEG-chain attached to XO) was examined by using ^{125}I-labeled derivatives. Both radiolabeled native XO and PEG-XO-high were prepared by the chloramine-T method. S-180 tumor cells (2×10^6 cells) were implanted s.c. in the dorsal skin of ddY mice. The organ distribution study was performed on days 7–10 after tumor inoculation, when the tumors were 5–7 mm in diameter but contained no necrotic region.

^{125}I-Labeled native XO or PEG-XO-high was administered to mice via the tail vein (0.1 ml/mouse). After 24 h, mice were killed; blood samples were drawn by cardiac puncture, and mice were then subjected to reperfusion with 5 ml of saline containing heparin (4 units/ml) to remove blood components in the blood vessels of the tissues. Tumor tissue as well as normal tissues including brain, liver, spleen, muscle, heart, lung, colon, and kidney were collected and weighed. The radioactivities of these tissues were measured by use of a gamma counter.

XO Activity in Various Tissues and Organs. The tissue distribution of the enzyme activity of PEG-XO-high and native XO was measured. PEG-XO-high was injected i.v. into mice bearing S-180 tumor. After 24 or 96 h, mice were killed; blood samples were drawn by cardiac puncture, and then mice were subjected to reperfusion as described above. Blood samples were then centrifuged at $3000 \times g$ for 5 min to obtain plasma samples. Tumor tissue and tissues from liver, spleen, and kidney were collected, weighed, and homogenized in 50 mM sodium phosphate buffer (pH 7.4) containing 10 mM DTT, 2 mM EDTA, 2 mM amidinophenylmethanesulfonyl fluoride, and 0.5 μg/ml leupeptin. These homogenates were centrifuged, and the supernatants were collected. The plasma samples and the supernatants were applied to size exclusion chromatography (column of 1.0×30 cm) with FPLC (Pharmacia) as described above. The fraction that eluted between 10 and 12 ml of elution volume, corresponding to PEG-XO-high, was collected, and XO activity was measured by the fluorescence method as described (see above).

In Vivo Antitumor Activity of PEG-XO

The same mice bearing palpable S-180 tumors described above were used to examine the therapeutic efficacy of the treatment. Native XO or PEG-XO-high was injected i.v. according to the time schedule indicated (see Fig. 3). Hypoxanthine was administered i.p. twice daily at 33 mg/kg body weight from days 11 to 21 after tumor inoculation, at 12 h or later after native XO or PEG-XO-high injection. Tumor sizes, by longitudinal cross section (L) and transverse section (W), were estimated, and tumor volume was defined by the formula $(L \times W^2)/2$.

Statistical Analysis

Student's t test was used to determine significance between each experimental group. The difference was considered to be statistically significant when $P < 0.05$.

RESULTS

Synthesis and Characterization of PEG-XO. The reaction between succinimidyl PEG and XO was completed at 8°C within 30 min (time course of reaction; not shown). The physicochemical and biochemical characteristics of native XO and PEG-XO are summarized in Table 1. The different feed molar ratios of succinimidyl PEG at 1.2 or 6.7 per mol of ϵ-amino groups of lysine in XO resulted in 17% (PEG-XO-low) or 49% (PEG-XO-high) conjugation to the amino groups in XO, respectively. The molecular sizes of these PEG-XO conjugates were M_r 383,000 and M_r 543,000, respectively, as estimated by the degree of conjugation, *i.e.,* loss of amino groups as determined by the TNBS assay. The increase in the apparent molecular size of XO in aqueous media after PEG conjugation was also

Table 1 *Physicochemical and biochemical characteristics of native XO and PEG-XO*

	Feed ratio[a] (PEG/amino group)	No. of free amino groups[b]	% conjugated[b] based on [R-NH_2]	M_w[c]	M_p[d]	XO activity (units/mg protein)
Native XO		89	0	298,000	298,000	2.12
PEG-XO-low	1.2	73.9	17	383,000	580,000	2.40
PEG-XO-high	6.7	45.4	49	543,000	850,000	1.15

[a] Molar ratio.
[b] Determined by the TNBS method.
[c] Molecular sizes were calculated from the loss of amino groups and attached PEG.
[d] Peak molecular sizes were estimated by means of size exclusion chromatography, using globular proteins as molecular size markers for calibration.

demonstrated by means of size exclusion chromatography (Fig. 1*A*). The peak molecular sizes of PEG-XO conjugates, which were estimated by using a calibration curve with protein molecular size markers, were M_r 580,000 and M_r 850,000 for PEG-XO-low and PEG-XO-high, respectively (Table 1). These values appeared larger than those for PEG-XO conjugates calculated by the conjugated numbers of PEG chains, perhaps because of the highly hydrated expanding structure of PEG chains on the molecular surface of XO compared with the compact globular protein markers being used, with a resultant increase in Stokes radius in aqueous media.

We then investigated *in vivo* stability of PEG-XO-high with respect to structural integrity and enzyme activity. Fig. 1, *B* and *C*, shows XO activity detected in plasma (Fig. 1*B*) and in tumor tissue homogenate (Fig. 1*C*) obtained from mice given PEG-XO-high or native XO via the tail vein. In plasma from mice injected with PEG-XO-high, significantly high XO activity was detected only in the high molecular weight fractions (10–13 ml), corresponding to the elution volume of PEG-XO-high (Fig. 1*A*). Similarly, we found a significant increase in XO activity corresponding to PEG-XO-high in the tumor tissue homogenate (Fig. 1*C*). These results suggest that PEG-XO-high is delivered to tumor tissue as active enzyme without detectable degradation products having a molecular size between PEG-XO-high and native XO.

PEG-XO-low showed a slight increase in enzyme activity (110%) compared with native XO (Table 1). We found previously that PEG conjugation of bilirubin oxidase reduces the Michaelis constant (K_m) to ~30% of that of native enzyme, indicating higher affinity caused by the introduction of the amphiphilic PEG chain (30). Similar effect of PEG conjugation may operate for PEG-XO, because hypoxanthine, a substrate for XO, is also a hydrophobic molecule. PEG-XO-high, even after modification of 49% of amino groups, retained 54% of the original enzyme activity of native XO *in vitro*. All experiments described below were carried out with PEG-XO-high, henceforth referred to as PEG-XO.

***In Vivo* Distribution of PEG-XO after i.v. Injection.** To see the effect of PEG conjugation with XO on body distribution of PEG-XO, we measured the *in vivo* distribution of ^{125}I-labeled native XO and PEG-XO after i.v. injection in tumor-bearing mice. The results were expressed as a ratio of radioactivity of PEG-XO to that of native XO detected in each organ (Fig. 2*A*). PEG conjugation significantly increased both blood and tumor accumulation of PEG-XO compared with that of native XO. PEG-XO showed 2.8 and 5.1 times higher accumulation in tumor and blood, respectively, compared with native XO 24 h after injection. The radioactivities of PEG-XO detected in the heart, muscle, and colon were only 15, 10, and 9% of that of tumor (Fig. 2*B*). Vital organs such as the kidney, liver, brain, and lung did not capture PEG-XO as effectively as native XO. These results suggest that PEG conjugation of XO resulted in a preferential increase in blood and tumor accumulation.

Tumor accumulation of PEG-XO was further investigated by measuring enzyme activity of PEG-XO at 24 or 96 h after i.v. injection. As

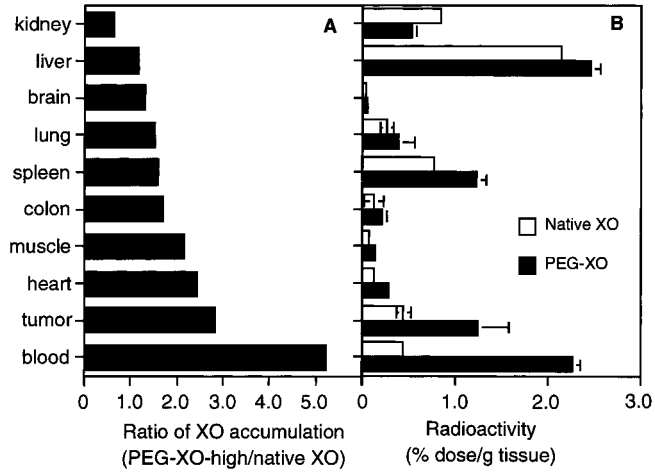

Fig. 2. Tissue distribution of native XO and PEG-XO-high in tumor-bearing mice. Radiolabeled native XO or PEG-XO-high was injected i.v. (n = 3). After 24 h, the radioactivities of organs and tissues, including tumor tissue, were measured. In *A*, the ratio of radioactivity of PEG-XO-high/native XO is shown. In *B*, radioactivities in various organs and tumor tissue are shown. Distribution of PEG-XO increased in most organs except the kidney, liver, brain, and lung. *Bars*, SE.

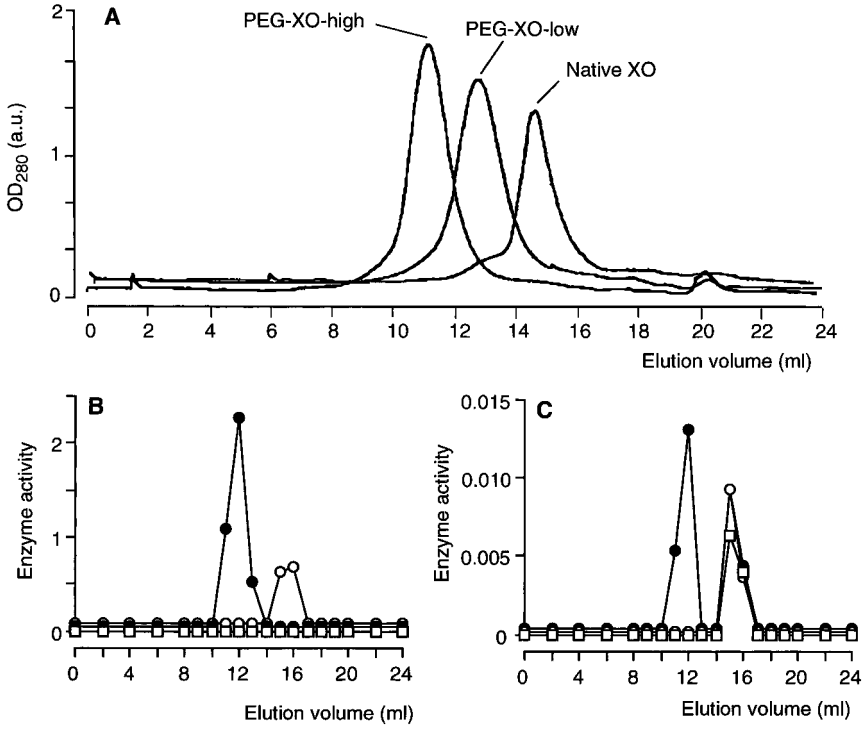

Fig. 1. Size exclusion chromatography of XO derivatives by use of FPLC; the column was Pharmacia's Superose 6 HR (10-mm inside diameter × 30 cm long); the elution buffer was 50 mM sodium phosphate buffer (pH 7.4). *A*, FPLC profiles of authentic samples (native XO and PEG-XO conjugates) detected at 280 nm. *B*, XO activities in plasma from mice injected with vehicle (control, □), native XO (0.4 unit/mouse, ○), or PEG-XO-high (0.4 unit/mouse, ●), at 24 h after injection. XO enzyme activity was expressed as units of isoxanthopterin formation (nmol isoxanthopterin/min·ml plasma). See text for details. *C*, XO activities in tumor tissue homogenate from mice injected with vehicle (control, □), native XO (0.4 unit/mouse, ○), or PEG-XO-high (0.4 unit/mouse, ●), at 24 h after injection. XO enzyme activity was expressed as units of isoxanthopterin formation (nmol isoxanthopterin/min·mg protein).

Table 2 *Enzyme activity of PEG-XO detected by FPLC chromatography of the tissues after i.v. injection of XO*

PEG-XO (0.45 unit/mouse) was injected i.v. Values are means ± SD ($n = 3$).

Tissue	Enzyme activity (pmol isoxanthopterin/min · mg protein)			
	Endogenous XO without XO injection[a]	Native XO, 24 h	PEG-XO, 24 h (activity at high M_w fraction[b])	PEG-XO, 96 h (activity at high M_w fraction)
Blood	7.3 ± 2.7	75.0[c,d]	245.6 ± 88.63[e]	11.32 ± 5.00[e]
Liver	130.2 ± 16.1	n.d.[f]	7.09 ± 4.04	0.84 ± 0.24
Kidney	30.2 ± 2.5	n.d.	9.15 ± 2.64	0.52 ± 0.27
Spleen	14.5 ± 2.4	n.d.	3.75 ± 1.61	0.13 ± 0.11
Tumor	36.4 ± 2.1	44.2[c,d]	35.4 ± 3.64[e]	2.93 ± 0.71[e]

[a] Substantial XO activity is detectable as endogenous XO, showing the size of native bovine XO.
[b] In these animals, XO activity detected at the size of native XO, when PEG-XO was injected i.v., was almost the same as that without XO injection (compare footnote *a*).
[c] Average of duplicate measurements.
[d] This value consists of both endogenous XO and native XO injected i.v.
[e] $P < 0.01$ blood and tumor *versus* liver, kidney, and spleen.
[f] ND, not determined.

shown in Fig. 1, *B* and *C*, enzyme activity of PEG-XO in organs and tissues can be quantified separately from that of endogenous XO by fractionation of samples with use of the FPLC system. Table 2 summarizes enzyme activities of PEG-XO as well as endogenous native XO detected in major organs. The liver is the organ with the most abundant endogenous native XO, with 3.6 times more endogenous XO than tumor (Table 2). In contrast, the highest enzyme activity of PEG-XO was detected in tumor compared with other organs and tissues except blood; the activity of PEG-XO in tumor was 5.0, 3.9, and 9.4 times higher than that in the liver, kidney, and spleen, respectively.

***In Vivo* Antitumor Activity of PEG-XO.** Native XO or PEG-XO was first administered i.v., and after the lapse of adequate time (*e.g.*, 12 h after each administration) to allow accumulation of XO in the tumor, its substrate hypoxanthine was administered by bolus i.p. injection. Thus, enzyme reactions should take place predominantly in tumor tissue, because of the accumulation of enzyme in the tumor, and hence systemic side effects would be reduced.

As shown in Fig. 3, significant suppression of tumor growth was observed in mice given PEG-XO and hypoxanthine. Growth suppression continued to at least up to 52 days after tumor inoculation, which was 36 days after the last PEG-XO administration and 30 days after the last hypoxanthine administration. Complete regression of tumor growth was observed in three of seven tumors in mice after treatment with PEG-XO and hypoxanthine. In contrast, similar treatment by native XO showed no significant reduction in tumor growth (Fig. 3). Fig. 4 shows body weight changes in mice receiving different treatments. No significant loss of body weight was observed in the group treated with PEG-XO plus hypoxanthine *versus* the group without tumor and the group given no treatment; tumor growth appeared to account for the increased body weight in control mice with tumor. A tumor mass of 12 × 24 mm would weigh about 1 g. These findings suggest that the systemic side effect of PEG-XO/hypoxanthine treatment was very small, if any at all. Endogenous XO is known to exist in most organs such as the liver, which are equipped with many free radical scavengers such as glutathione, peroxidases, and superoxide dismutase. Administration of PEG-XO alone or hypoxanthine alone showed no effect on growth of S-180 tumor (Fig. 3). These data suggest that ROS generated by PEG-XO plus hypoxanthine exert an antitumor effect.

DISCUSSION

The present study demonstrates that chemical conjugation of PEG to XO improved therapeutic potential of XO to inhibit tumor growth *in vivo*. It has generally been recognized that PEG-conjugation reduces immunogenicity and antigenicity of proteins (31). In addition, PEG is nontoxic, so that PEG and PEG-protein conjugates were approved by the Food and Drug Administration for clinical use such as PEG-asparaginase (32). Similarly, PEG-XO would become useful in a clinical setting.

It was reported previously that XO showed cytotoxic activity against cancer cells in model systems both *in vitro* (33) and *in vivo* (2, 3). In those studies, ROS generated from the reaction of XO with its substrate, hypoxanthine, were found to be a cytotoxic principle, as confirmed by inhibitory actions of superoxide dismutase (3) and catalase (3, 33) against XO-generated cytotoxicity.

As shown in Table 2, normal organs did not entrap PEG-XO, and only endogenous XO was found. The difference in molecular size of PEG-XO and XO was identified by using FPLC (Fig. 1). The amounts of PEG-XO in most of the normal organs and tissues were far below (<10–20%) the level of endogenous native XO. Thus, toxicity caused by PEG-XO is anticipated to be very small, if any. From the toxicity and body weight profile, the drawback of native XO (*i.e.*, binding to the vascular wall) appears to be prevented to a great extent by polymer

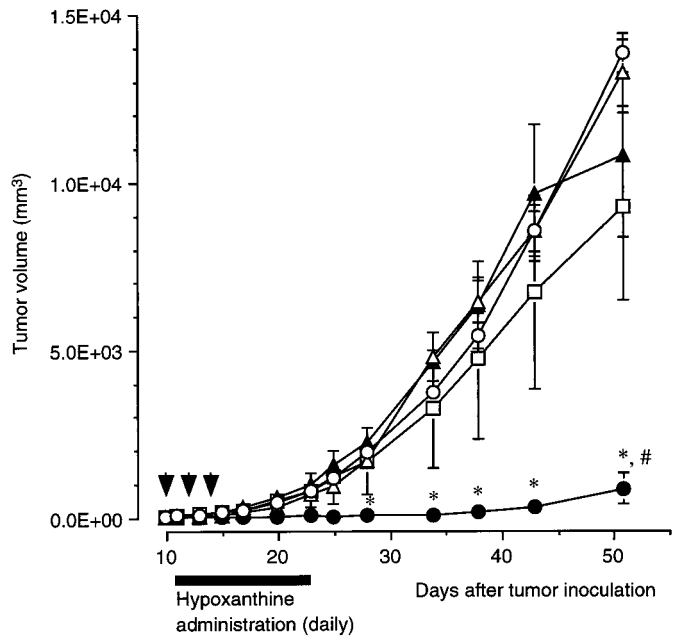

Fig. 3. Antitumor activity of PEG-XO with or without hypoxanthine administration. *Arrowheads*, administration of native XO or PEG-XO (0.6 unit/mouse for the first and second administrations and 0.2 unit/mouse for the third administration). Hypoxanthine was administered at 33 mg/kg body weight i.p. twice daily from days 11 to 21 after tumor inoculation, at 12 h or later after XO or PEG-XO injection. ○, control without any drug in S-180 tumor-bearing mice; ●, PEG-XO plus hypoxanthine; ▲, native XO plus hypoxanthine; △, PEG-XO alone; □, hypoxanthine alone. Data are means ($n = 6–8$); *bars*, SE. *, $P < 0.001$. #, The complete regression of tumor growth was observed in three of seven tumors in mice after treatment with PEG-XO plus hypoxanthine. See text for details.

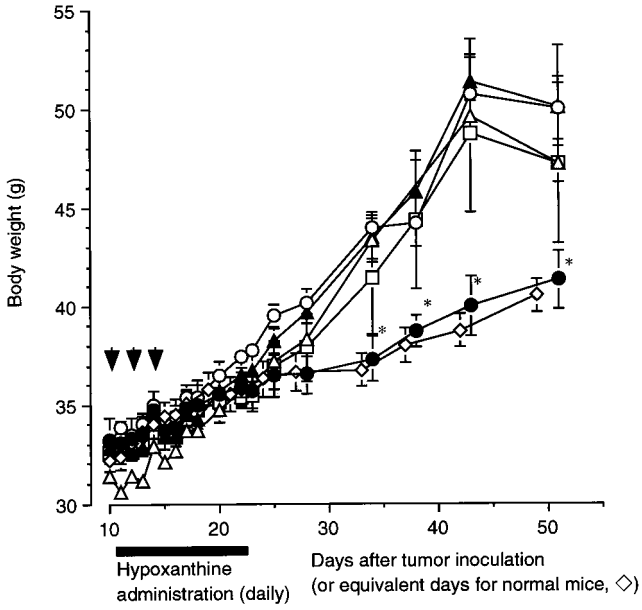

Fig. 4. Body weight changes in ddY mice treated with native XO, PEG-XO, or hypoxanthine. The treatment protocol is the same as that for Fig. 3. ○, control mice bearing S-180 tumor without any drug; ●, PEG-XO plus hypoxanthine; ▲, native XO plus hypoxanthine; △, PEG-XO alone; □, hypoxanthine alone; ◇, control mice without tumor and no drugs. Data are means ($n = 4$); *bars*, SE. *, $P < 0.05$ for only group ● compared with all other treatments. No difference between groups ● and ◇ was observed. Among the groups (○, ▲, △, □), no significant difference was observed, regardless of error bars.

conjugation of XO (PEG-XO). PEG chains linked to ϵ-amino groups would interfere with the interaction between XO and endothelium because of the large exclusion volume of PEG in an aqueous solution (34). Pharmacokinetic studies showed that PEG conjugation significantly increased the blood concentration of circulating XO but did not show as great a distribution to other normal organs compared with native XO (Fig. 2). These phenomena were observed with other polymer conjugates as well as gelatin conjugates (14, 35). Low plasma levels of native XO are perhaps attributable to adsorption to the endothelial surface of blood vessels, because the large molecular size of XO (M_r 298,000) prevents its clearance by the kidney.

In contrast to its accumulation in normal organs such as the liver, kidney, and spleen, PEG-XO exhibited highly tumoritropic accumulation (Fig. 2 and Table 2). These results are consistent with our previous findings and those of others that macromolecules preferentially accumulate in solid tumor (13–24). The phenomenon of tumor-selective uptake might be explained by the EPR effect of macromolecules and lipids, as observed for a variety of polymeric drugs in solid tumors (13–24, 26, 36, 37). The EPR effect is attributed to multiple causes unique to solid tumor, *i.e.*: (*a*) a number of vascular permeability-enhancing factors such as NO (22, 36–38), bradykinin (22, 37, 39), prostaglandin (22), and vascular endothelial growth factor/vascular permeability factor (40) are produced in tumors; (*b*) high-level angiogenesis/hypervasculature, *i.e.*, high vascular density (41, 42), would result in more extravasation caused by the above mediators; (*c*) defective (thus leaky) vascular architecture is found in tumors (43, 44); and (*d*) lymphatic drainage from tumor tissue interstitium is deficient (13, 18, 21).

The concept of the EPR effect is now widely recognized as a rational strategy for selective targeting of tumors (25). For instance, SMANCS, which is poly(styrene-co-maleic acid half *n*-butylate)-conjugated neocarzinostatin (45), dissolved in the lipid contrast agent Lipiodol (18), shows a tumor:blood ratio of >1000 when administered intraarterially. SMANCS/Lipiodol has been used clinically to treat hepatoma in Japan experimentally since 1983 (15, 23, 24, 46) and was approved by the Japanese government in 1996. On the basis of the EPR effect, several polymer therapeutics were developed; *N*-(2-hydroxypropyl)-methacrylamide copolymer-doxorubicin conjugate (PK1) completed Phase I/II clinical trials (20, 25, 26), and many more agents are presently in Phase I clinical trials.

As we reported previously, the EPR effect is found for macromolecules with good biocompatibility and molecular sizes larger than M_r ~40,000 (13, 20, 21). It should operate for PEG-XO, with a molecular size of M_r >40,000 (Table 1) and biocompatibility. Recently, it was reported that administration of both native XO and hypoxanthine produced an antitumor effect against rabbit VX2 carcinoma (3); however, to accomplish effective tumor-selective delivery of XO, it was required to use a catheter whose tip was placed upstream of the tumor-feeding artery covering the tumor area, via the femoral artery. This strategy avoids nonspecific vascular uptake, and the first-path effect plus the EPR effect will capture XO effectively at the tumor site. However, our study reported here demonstrated that native XO administered systemically via the tail vein was not effective in the present solid tumor model, as explained by the fact that adsorption of native XO on blood vessel walls would have resulted in decreased efficacy of delivery to tumor.

The mechanism of antitumor action of PEG-XO is considered to involve ROS generation because its antitumor activity requires coadministration of hypoxanthine, whereas PEG-XO or hypoxanthine alone did not produce any appreciable antitumor effect (Fig. 3). This notion is supported by the fact that the treatment of tumor cells by native XO and hypoxanthine increased the level of oxidized lipids, a marker of oxidative cell damage (3). ROS can cause damage in variety of biologically important molecules, such as membrane lipids, enzymes, proteins, RNA, and DNA, and consequently lead to cell death (33). Interestingly, most previous reports have suggested that levels of antioxidant enzymes such as superoxide dismutase and catalase are low in tumors (47, 48). This notion may explain the susceptibility of S-180 solid tumor to the cytotoxic action of ROS generated by PEG-XO.

Because of the highly cytotoxic nature of ROS, ROS other than O_2^- such as singlet oxygen could show antitumor activity. Several photosensitizers are known to produce singlet oxygen by light irradiation, and therefore used to treat tumor. Interestingly, polymer conjugated photosensitizers exhibited preferential tumor accumulation and more potent antitumor activity compared with free drugs, which might be attributable to the EPR effect by polymer conjugation (49, 50). Thus, polymer conjugates that generate ROS would become promising area of anticancer therapeutics.

In addition to the direct cytotoxic effect of ROS, the effect of O_2^- on tumor blood flow may be of considerable interest. As mentioned in the "Introduction," NO plays a crucial role in the maintenance of blood flow (8). Because O_2^- will react rapidly with NO (51), NO may be depleted by excessive O_2^- production. We have found that NO is produced in excess in solid tumors (22, 37, 38) and that NO promotes tumor growth and the EPR effect (22, 36–38) as well as blood flow. These data indicate that tumor blood flow may be greatly impaired when O_2^- is generated by PEG-XO and hypoxanthine, and hence the growth of tumor could be suppressed or could even lead to necrosis. In addition, the reaction product of NO and O_2^-, $ONOO^-$, is a potent cytotoxic agent as well as apoptosis inducer (52). Thus, NO metabolites have multiple mechanisms of action. These notions need further investigation.

Very recently, we found that tumor cells (AH136B hepatoma) express the inducible type of heme oxygenase (HO-1) extensively, and we showed that HO-1 plays a protective role in tumor growth against oxidative stress by generating a potent antioxidative component (bilirubin) from heme groups (53). Moreover, a specific inhibitor of HO-1 (zinc protoporphyrin IX) was found to induce significant suppression of tumor growth *in vivo* by inhibiting the antioxidative system (bilirubin formation) and concomitant elevation of oxidative stress caused by suppression of HO-1; it finally did lead to tumor regression (53).

In conclusion, we report here that separate injection of two nontoxic components (PEG-XO and substrate) resulted in tumor regression. Because of the EPR effect, tumor-selective accumulation of PEG-XO became possible, and subsequent injection of hypoxanthine selectively generated highly potent cytotoxic ROS in tumor tissue. Consequently, effective antitumor activity can be accomplished without any apparent toxicity in normal tissues or organs.

ACKNOWLEDGMENTS

We thank Dr. Tom Conners, London, for his encouraging discussion, profound knowledge, and valuable comments. We also thank Judith Gandy for editing, Rie Yoshimoto for typing, and Jun Fang for technical assistance.

REFERENCES

1. Fridovich, I. Quantitative aspects of the production of superoxide anion radical by milk xanthine oxidase. J. Biol. Chem., *245:* 4053–4057, 1970.
2. Haddow, A., De Lamirande, G., Bergel, F., Bray, R. C., and Gilbert, D. A. Anti-tumor and biochemical effects of purified bovine xanthine oxidase in C3H and C mice. Nature (Lond.), *182:* 1144–1146, 1958.
3. Yoshikawa, T., Kokura, S., Tainaka, K., Naito, Y., and Kondo, M. A novel cancer therapy based on oxygen radicals. Cancer Res., *55:* 1617–1620, 1995.
4. Bray, R. C., and Swann, J. C., Moribudenum-containing enzymes. Struct. Bonding, *11:* 107–144, 1972.
5. Yen, H. C., Oberley, T. D., Vichitbandha, S., Ho, Y. S., and St. Clair, D. K. The protective role of manganese superoxide dismutase against Adriamycin-induced acute cardiac toxicity in transgenic mice. J. Clin. Investig., *98:* 1253–1260, 1996.
6. Adachi, T., Fukushima, T., Usami, Y., and Hirano, K. Binding of human xanthine oxidase to sulphated glycosaminoglycans on the endothelial-cell surface. Biochem. J., *289:* 523–527, 1993.
7. Radi, R., Rubbo, H., Bush, K., and Freeman, B. A. Xanthine oxidase binding to glycosaminoglycans: kinetics and superoxide dismutase interaction of immobilized xanthine oxidase-heparin complexes. Arch. Biochem. Biophys., *339:* 125–135, 1997.
8. Houston, M., Estevez, A., Chumley, P., Aslan, M., Marklund, S., Parks, D. A., and Freeman, B. A. Binding of xanthine oxidase to vascular endothelium. Kinetic characterization and oxidative impairment of nitric oxide-dependent signaling. J. Biol. Chem., *274:* 4985–4994, 1999.
9. Moncada, S., Palmer, R. M., and Higgs, E. A. Nitric oxide: physiology, pathophysiology, and pharmacology. Pharmacol. Rev., *43:* 109–142, 1991.
10. Nakazono, K., Watanabe, N., Matsuno, K., Sasaki, J., Sato, T., and Inoue, M. Does superoxide underlie the pathogenesis of hypertension? Proc. Natl. Acad. Sci. USA, *88:* 10045–10048, 1991.
11. Bruder, G., Jarasch, E-D., and Heid, H. W. High concentrations of antibodies to xanthine oxidase in human and animal sera: molecular characterization. J. Clin. Investig., *74:* 783–794, 1984.
12. Ng, Y. L., and Lewis, W. H. Circulating immune complexes of xanthine oxidase in normal subjects. Br. J. Biomed. Sci., *51:* 124–127, 1994.
13. Matsumura, Y., and Maeda, H. A new concept for macromolecular therapeutics in cancer chemotherapy: mechanism of tumoritropic accumulation of proteins and the antitumor agent SMANCS. Cancer Res., *46:* 6387–6392, 1986.
14. Maeda, H., and Kojima, Y. Polymer-drug conjugates. *In:* R. Arshady (ed.), Desk Reference of Functional Polymers: Synthesis and Application, pp. 753–767. Washington, DC: American Chemical Society, 1997.
15. Maeda, H. SMANCS and polymer-conjugated macromolecular drugs: advantages in cancer chemotherapy. Adv. Drug Delivery Rev., *6:* 181–202, 1991.
16. Maeda, H., and Matsumura, Y. Tumoritropic and lymphotropic principles of macromolecular drugs. Crit. Rev. Ther. Drug Carrier Syst., *6:* 193–210, 1989.
17. Li, C. J., Miyamoto, Y., Kojima, Y., and Maeda, H. Augmentation of tumour delivery of macromolecular drugs with reduced bone marrow delivery by elevating blood pressure. Br. J. Cancer, *67:* 975–980, 1993.
18. Iwai, K., Maeda, H., and Konno, T. Use of oily contrast medium for selective drug targeting to tumor: enhanced therapeutic effect and X-ray image. Cancer Res., *44:* 2115–2121, 1984.
19. Iwai, K., Maeda, H., Konno, T., Matsumura, Y., Yamashita, R., Yamasaki, K., Hirayama, S., and Miyauchi, Y. Tumor targeting by arterial administration of lipids: rabbit model with VX2 carcinoma in the liver. Anticancer Res., *7:* 321–328, 1987.
20. Seymour, L. W., Miyamoto, Y., Maeda, H., Brereton, M., Strohalm, J. Ulbrich, K., and Duncan, R. Influence of molecular weight on passive tumour accumulation of a soluble macromolecular drug carrier. Eur. J. Cancer, *31:* 766–770, 1995.
21. Noguchi, Y., Wu, J., Duncan, R., Strohalm, J., Ulbrich, K., Akaike, T., and Maeda, H. Early phase tumor accumulation of macromolecules: a great difference in clearance rate between tumor and normal tissues. Jpn. J. Cancer Res., *89:* 307–314, 1998.
22. Wu, J., Akaike, T., and Maeda, H. Modulation of enhanced vascular permeability in tumors by a bradykinin antagonist, a cyclooxygenase inhibitor, and a nitric oxide scavenger. Cancer Res., *58:* 159–165, 1998.
23. Konno, T., Maeda, H., Iwai, K., Maki, S., Tashiro, S., Uchida, M., and Miyauchi, Y. Selective targeting of anti-cancer drug and simultaneous image enhancement in solid tumors by arterially administered lipid contrast medium. Cancer (Phila.), *54:* 2367–2374, 1984.
24. Seymour, L. W., Olliff, S. P., Poole, C. J., De Takats, P. G., Orme, R., Ferry, D. R., Maeda, H., Konno, T., and Kerr, D. J. A novel dosage approach for evaluation of SMANCS [poly-(styrene-co-maleyl-half-*n*-butylate)-neocarzinostatin] in the treatment of primary hepatocellular carcinoma. Int. J. Oncol., *12:* 1217–1223, 1998.
25. Muggia, F. M. Doxorubicin-polymer conjugates: further demonstration of the concept of enhanced permeability and retention. Clin. Cancer Res., *5:* 7–8, 1999.
26. Vasey, P. A., Kaye, S. B., Morrison, R., Twelves, C., Wilson, P., Duncan, R., Thomson, A. H., Murray, L. S., Hilditch, T. E., Murray, T., Burtles, S., Fraier, D., Frigerio, E., and Cassidy, J. Phase I clinical and pharmacokinetic study of PK1 (HPMA copolymer doxorubicin): first member of a new class of chemotherapeutic agents-drug-polymer conjugates. Clin. Cancer Res., *5:* 83–94, 1999.
27. Fields, R. The rapid determination of amino groups with TNBS. Methods Enzymol., *25:* 464–468, 1972.
28. Hunt, J., and Massey, V. Purification and properties of milk xanthine dehydrogenase. J. Biol. Chem., *267:* 21479–21485, 1992.
29. Akaike, T., Ando, M., Oda, T., Doi, T., Ijiri, S., Araki, S., and Maeda, H. Dependence on O_2^- generation by xanthine oxidase of pathogenesis of influenza virus infection in mice. J. Clin. Investig., *85:* 739–745, 1990.
30. Maeda, H., Kimura, M., Sasaki, I., Hirose, Y., and Konno, T. Toxicity of bilirubin and detoxification by PEG-bilirubin oxidase conjugate: a new tactic for treatment of jaundice. *In:* J. M. Harris (ed.), Poly(ethylene glycol) Chemistry: Biotechnical and Biomedical Applications, pp. 153–169. New York: Plenum Publishing Corp., 1992.
31. Abuchowski, A., van Es, T., Palczuk, N. C., and Davis, F. F. Alteration of immunological properties of bovine serum albumin by covalent attachment of polyethylene glycol. J. Biol. Chem., *252:* 3578–3581, 1977.
32. Wada, H., Imamura, I., Sako, M., Katagiri, S., Tarui, S., Nishimura, H., and Inada, Y. Antitumor enzyme: polyethylene glycol-modified asparaginase. Ann. NY Acad. Sci., *613:* 95–108, 1990.
33. Halliwell, B., and Gutteridge, J. M. Oxygen toxicity, oxygen radicals, transition metals and disease. Biochem. J., *219:* 1–14, 1984.
34. Harris, J. M. Introduction to biotechnical and biomedical applications of poly(ethylene glycol). *In:* J. M. Harris (ed.), Poly(ethylene glycol) Chemistry: Biotechnical and Biomedical Applications, pp. 1–14. New York: Plenum Publishing Corp., 1992.
35. Kojima, Y., Akaike, T., Sato, K., Maeda, H., and Hirano, T. Polymer conjugation to Cu, Zn-SOD and suppression of hydroxyl radical generation on exposure to H_2O_2: improved stability of SOD *in vitro* and *in vivo*. J. Bioactive Compatible Polymers, *11:* 169–190, 1996.
36. Maeda, H., Noguchi, Y., Sato, K., and Akaike, T. Enhanced vascular permeability in solid tumor is mediated by nitric oxide and inhibited by both new nitric oxide scavenger and nitric oxide synthase inhibitor. Jpn. J. Cancer Res., *85:* 331–334, 1994.
37. Maeda, H., Akaike, T., Wu, J., Noguchi, Y., and Sakata, Y. Bradykinin and nitric oxide in infectious disease and cancer. Immunopharmacology, *33:* 222–230, 1996.
38. Doi, K., Akaike, T., Horie, H., Noguchi, Y., Fujii, S., Beppu, T., Ogawa, M., and Maeda, H. Excessive production of nitric oxide in rat solid tumor and its implication in rapid tumor growth. Cancer (Phila.), *77:* 1598–1604, 1996.
39. Matsumura, Y., Maeda, H., and Kato, H. Degradation pathway of kinins in tumor ascites and inhibition by kininase inhibitors: analysis by HPLC. Agents Actions, *29:* 172–180, 1990.
40. Senger, D. R., Galli, S. J., Dvorak, A. M., Perruzzi, C. A., Harvey, V. S., and Dvorak, H. F. Tumor cells secrete a vascular permeability factor that promotes accumulation of ascites fluid. Science (Washington DC), *219:* 983–985, 1983.
41. Folkman, J. Tumor angiogenesis: therapeutic implications. N. Engl. J. Med., *285:* 1182–1186, 1971.
42. Folkman, J. Angiogenesis in cancer, vascular, rheumatoid and other disease. Nat. Med., *1:* 27–31, 1995.
43. Ohtani, H., and Sasano, N. Microvascular changes in the stroma of human colorectal carcinomas: ultrastructural histochemical study. Jpn. J. Cancer Res., *80:* 360–365, 1989.
44. Suzuki, M., Takahashi, T., and Sato, T. Medial regression and its functional significance in tumor-supplying host arteries. A morphometric study of hepatic arteries in human livers with hepatocellular carcinoma. Cancer (Phila.), *56:* 444–450, 1987.
45. Maeda, H., Ueda, M., Morinaga, T., and Matsumoto, T. Conjugation of poly(styrene-co-maleic acid) derivatives to the antitumor protein neocarzinostatin: pronounced improvements in pharmacological properties. J. Med. Chem., *28:* 455–461, 1985.
46. Konno, T., Maeda, H., Iwai, K., Tashiro, S., Maki, S., Morinaga, T., Mochinaga, M., Hiraoka, T., and Yokoyama, I. Effect of arterial administration of high molecular weight anticancer agent SMANCS with lipid lymphographic agent on hepatoma: a preliminary report. Eur. J. Cancer Clin. Oncol., *19:* 1053–1065, 1983.
47. Sun, Y. Free radicals, antioxidant enzymes, and carcinogenesis. Free Radical Biol. Med., *8:* 583–599, 1990.
48. Sato, K., Ito, K., Kohara, H., Yamaguchi, Y., Adachi, K., and Endo, H. Negative regulation of catalase gene expression in hepatoma cells. Mol. Cell. Biol., *12:* 2525–2533, 1992.
49. Krinick, N. L., Sun, Y., Joyner, D., Spikes, J. D., Straight, R. C., and Kopecek, J. A polymeric drug delivery system for the simultaneous delivery of drugs activatable by enzymes and/or light. J. Biomater. Sci. Polym. Ed., *5:* 303–324, 1994.
50. Tabata, Y., Murakami, Y., and Ikada, Y. Photodynamic effect of polyethylene glycol-modified fullerene on tumor. Jpn. J. Cancer Res., *88:* 1108–1116, 1997.
51. Pryor, W. A., and Squadrito, G. L. The chemistry of peroxynitrite: a product from the reaction of nitric oxide with superoxide. Am. J. Physiol., *268:* L699–L722, 1995.
52. Szabo, C., and Ohshima, H. DNA damage induced by peroxynitrite: subsequent biological effects. Nitric Oxide, *1:* 373–385, 1997.
53. Doi, K., Akaike, T., Fujii, S., Tanaka, S., Ikebe, N., Beppu, T., Shibahara, S., Ogawa, M., and Maeda, H. Induction of heme oxygenase-1 by nitric oxide and ischemia in experimental solid tumors and implications for tumor growth. Br. J. Cancer, *80:* 1945–1954, 1999.